

The structure of amorphous silicon telluride

Part 1 X-ray diffraction investigation

F. R. L. SCHOENING*

Department of Physics, University of the Witwatersrand, Johannesburg, South Africa

The radial distribution functions which were obtained from X-ray diffraction measurements of $\text{Te}_{78}\text{Si}_{22}$ and $\text{Te}_{87}\text{Si}_{13}$ between 6.5 and 470 K compared well with those calculated from a model based on the intersection of Te, Si chains, where Si is common to both chains. Si has four Te neighbours in tetrahedral coordination and Te has two neighbours. The mean-square displacements of the atoms were calculated from the widths of the peaks in the radial distribution function and from the Debye–Waller factor.

1. Introduction

Semiconducting chalcogenide glasses are interesting materials not only because they are of technological importance, but also because they are not intrinsic semiconductors and are not doped. Tellurium–silicon alloys have been selected for a detailed study because they belong to a simple binary system which forms glasses easily. The covalent nature of the bonds in the Te–Te chains in the crystalline state added interest to the study of the Te–Te bond in the amorphous state.

There have been a number of recent investigations of the structure of amorphous $\text{Si}_x\text{Te}_{1-x}$. Hilton *et al.* [1], Bartsch and Just [2] and Bartsch *et al.* [3] have published X-ray radial distribution functions (RDFs) for the range $0.1 \leq x \leq 0.4$. Bartsch and co-workers concluded that Si tetrahedrally surrounded by Te and divalent Te were the most likely general features of the structure. Petersen *et al.* [4] measured and compared the microscopic physical properties of the crystalline phase Si_2Te_3 with the amorphous alloy ($0.02 \leq x \leq 0.25$), using infra-red transmission, differential thermal analysis and electron paramagnetic resonance. Their results agree with the structural features proposed by Bartsch *et al.* [2, 3]. The earlier X-ray work by Hilton *et al.* [1] is also in general agreement, although

there are some uncertainties about the inter-atomic distances.

Previous authors have based their conclusions about the probable structure on predicted and measured areas under the first and second peaks in the RDF. For multicomponent systems this approach cannot give more than a qualitative picture of the arrangements in the first and second coordination shells. A more quantitative result can be obtained by the direct comparison of the measured and predicted RDFs where the latter is calculated from the scattering expected from an assumed model. By checking the same model against different compositions and against X-ray and neutron diffraction results, further stringent tests are possible. For the purpose of establishing a better detailed structure of the nearest neighbour configuration the above approach was implemented in the present investigation. The neutron diffraction results are reported in Part 2 of this series.

In addition to the arrangement of the nearest neighbour atoms, diffraction experiments can give information about the thermal displacements of the atoms. This information can be obtained from the widths of the peaks in the RDF and from the Debye–Waller factor which affects the measured intensities. As this additional information appeared to be desirable, the diffraction measure-

*A large part of this research was done during the author's sabbatical leave with Professor H. Ruppertsberg at the Universität des Saarlandes.

ments were carried out between 6.5 and 470 K. The latter temperature is between the glass point and the crystallization temperature of $\text{Te}_{78}\text{Si}_{22}$ (78 at % Te, 22 at % Si).

Most of the work was done with $\text{Te}_{78}\text{Si}_{22}$ and some with $\text{Te}_{87}\text{Si}_{13}$. The results have been compared with a model of compositions $\text{Te}_{80}\text{Si}_{20}$ (SiTe_4) and $\text{Te}_{85.7}\text{Si}_{14.3}$ (SiTe_6) which were considered to be close enough to the specimen compositions for the present purpose. Both compositions are in the vicinity of a eutectic point which Bailey [5] has put between 80 and 90 at % Te.

2. Experimental procedure and data reduction

The specimen preparation was identical to that reported by Bartsch *et al.* [2, 3]. Some specimens were measured as prepared and others were stabilized and aged by suitable heat treatments. These treatments had negligible influence on the positions of the first and second peaks in the RDF but did affect the breadths of these peaks. As it was possible to pool data from different specimens of the same composition by making allowance for the different static displacement broadenings, the thermal history of the samples became less critical. All diffraction specimens were prepared by grinding the ingots and compacting the powders.

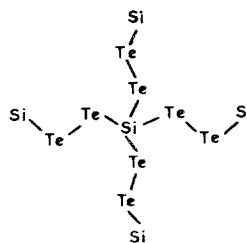
X-ray diffraction measurements, using crystal monochromated $\text{MoK}\alpha$ radiation, were carried out in reflection with different diffractometers. Observations at 170, 295, 400, 450, 470 K were done with a Seifert $\theta-\theta$ diffractometer at the University of Saarbrücken and at 295 and 6.5 K with an Oxford Instruments liquid He stage on a Philips diffractometer at the University of the Witwatersrand. The temperatures were determined by means of thermocouples and checked by measuring the lattice parameter of Ag powder deposited on the sample surface. It was estimated that the temperature of the diffracting material was known to $\pm 5^\circ\text{C}$, except for the low temperature where the temperature was known to $\pm 1\text{K}$. As this accuracy was sufficient for the present investigation, no attempts were made to refine the temperature measurements.

The standard data reduction procedure, e.g. Wagner [6], was followed except that no damping factor was applied before the Fourier inversion. This led to higher than usual ripples in the region below 2Å , but as similar ripples appear in the model calculations no experimental inaccuracy

was indicated. On the contrary, the absence of the ripples would have been suspicious.

3. Radial distribution function and model calculations

The model which was used to fit the RDF was similar to one mentioned by Bartsch and Just [2]. For Te_4Si the helical chain of Te atoms which exists in crystalline Te, has been modified by replacing every third Te by Si. Two chains are made to intersect each other by making one Si common to both chains. The intersection of a right-hand helical chain with a left-hand helix at 90° can lead to a nearly tetrahedrally coordinated Si atom. Each Si has four Te neighbours and each Te has one Si and one Te neighbour, thereby satisfying all bond requirements:



When intersecting two left- or right-handed helical chains and giving Si a tetrahedral coordination, the chains do not cross at 90° and interatomic distances around 3.4Å are obtained which can not be reconciled with the observed RDF. The amorphous structure is therefore obviously different from the crystalline structure which consists of either left- or right-handed helical chains and not both. The inability to separate into all left and all right regions could contribute to the remarkable stability of the amorphous state of these alloys.

The interatomic distances up to 6Å were calculated or taken from a mechanical model which was based on above considerations. As the atoms from one intersection do not fill the space up to 6Å radius, atoms from neighbouring intersections have been incorporated in the model. The distances were then adjusted in order to obtain a better fit with the RDF and to allow different bond lengths for Si-Te and Te-Te.

The procedure proposed by Warren [7], was used to calculate the RDF from the intensity which was expected from the proposed model. Random static displacements of the atoms from their ideal positions in the model were introduced until good fit with the observed RDF was ob-

TABLE I Interatomic distances within 6 Å radius.

SiTe ₄			SiTe (I) ₄ Te(II) ₂		
Atom	No. and type of neighbours	Distance* (Å)	Atom	No. and type of neighbours	Distance* (Å)
Si	4Te	2.62	Si	4Te	2.62
Si	4Te	4.18	Si	4Te	4.22
Si	4Te	5.5	Si	4Te	6.0
Si	4Si	6.0			
Te	1Si	2.62	Te (I)	1Si	2.62
Te	1Te	2.74	Te (I)	Te	2.79
Te	1Si	4.18			
Te	3Te	4.28	Te (I)	3Te	4.28
Te	1Si	5.3	Te (I)	1Te	4.35
Te	1Te	5.8	Te (I)	1Te	4.4
Te	4Te	6.0	Te (I)	1Te	5.6
Te	3Te	3.7	Te (I)	2Te	6.0
Te	3Te	4.0 [†]	Te (I)	1Si	6.0
Te	3Te	4.3	Te (II)	2Te	2.79
			Te (II)	2Si	4.22
			Te (II)	2Te	4.4
			Te	2Te	3.7
			Te	3Te	4.0 [†]

*Distances given to 3 significant figures were calculated, the remaining were taken from a model.

[†] Van der Waal's contacts between neighbouring helices.

tained. The broadening parameters expressed in half-height widths of a Gaussian distribution are 0.15 Å for the first peak and 0.35 Å for the second peak for SiTe₄ and 0.15 and 0.25 Å respectively for SiTe₆. The interatomic distances at 295 K are given in Table I and a comparison of calculated and observed RDF is shown in Fig. 1.

The model for SiTe₄ which is presented here in terms of the intersection of two helical chains, can just as well be described by the packing of SiTe₄

tetrahedra with proper allowance for the —Si—Te—Te—Si— bond configuration. However, the chain intersection offers a simpler description for alloys of lower Si concentration. For SiTe₆ every fourth Te is replaced by Si which again is common to two chains. In Fig. 2 this model is compared with the X-ray results for Te₈₇Si₁₃.

The idealized picture of the intersection of helical chains could lead to a highly ordered structure if rotation around the bonds was not allowed.

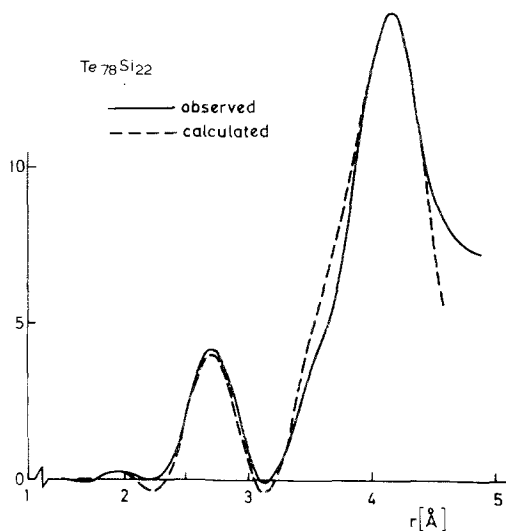


Figure 1 Observed and calculated RDF for Te₇₈Si₂₂.

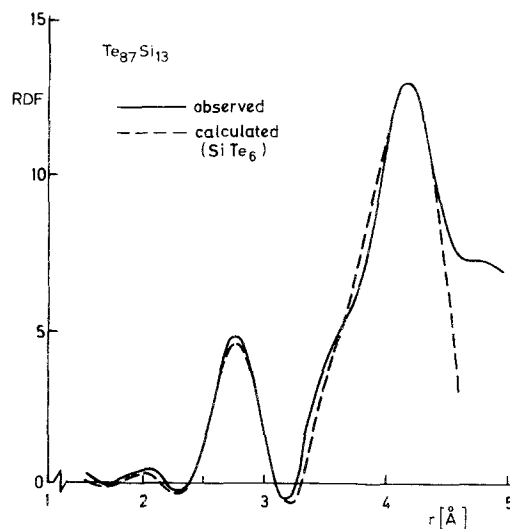


Figure 2 Observed and calculated RDF for Te₈₇Si₁₃.

Rotation around bonds must therefore be permitted for the chains to form a three-dimensional amorphous network.

4. Temperature broadening of the radial distribution function

The temperature broadening is small in comparison to the observed width of the peaks in the RDF. Measurements of the change of width with temperature are therefore heavily affected by experimental errors and by small variations in the static broadening in samples of the same composition. Consistent results could only be obtained after correction for this variation of the static broadening. After correction for termination effects, Temkin *et al.* [8], the remaining breadths are composed of static and thermal broadening. At a given temperature the differences between the breadths of samples of the same composition can therefore be attributed to static broadening. The static broadening of the samples was equalized at 300°C by assuming Gaussian profiles and adding or subtracting constant arbitrary amounts of static broadening at all temperatures. In Fig. 3 the square of the adjusted breadth at half-maximum is plotted against temperature.

The thermal mean-square fluctuations of the separations of the atoms in the first and second shells are given in Table II. Zero point vibrations are included in the data and it is assumed that

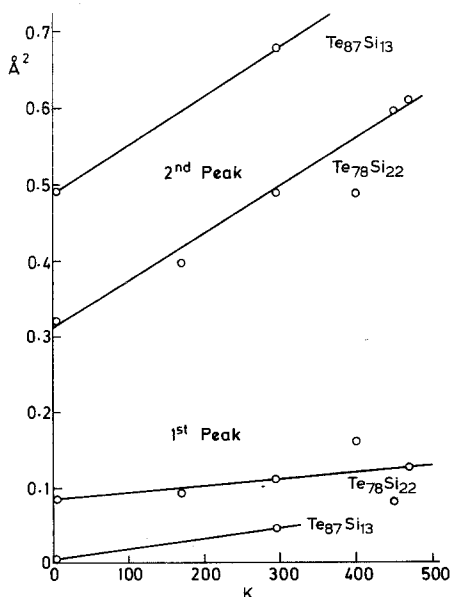


Figure 3 Mean-square breadths of the first and second peaks in the RDF as function of temperature.

2400

the thermal vibrations at 6.5 K are negligible. The data for 400 and 450 K are extremely erratic and have not been included in Table II. Whether this behaviour is due to changes occurring at the glass transition point, which lies between 400 and 450 K, is not clear at this stage.

Despite the large experimental errors, which are probably about 10%, Table II shows some obvious differences between the shells and between the samples. The *m*-s thermal vibration amplitudes are between 10 and 5 times smaller for the first shell than for the second shell and distinctly smaller for the first shell of Te₇₈Si₂₂ than for the first shell of Te₈₇Si₁₃.

The temperature changes of the breadths of the RDF peaks could also be caused by a differential expansion of the Te-Si and Te-Te distances. This could lead to increases or decreases of the breadths with temperature. Neutron diffraction results could give an answer to this question. The expansion of the first shell with temperature is shown in Fig. 4; again the value for 400 K is anomalous.

5. The Debye-Waller factor

The variation of $k(i(k) - 1)$ with temperature is shown in Fig. 5. Here k is $4\pi\lambda^{-1} \sin \theta$ and $i(k)$ is the structure factor or the interference function which is obtained from the observed intensities after normalization and elimination of the Compton scattering. It is obvious that the amplitudes of $k(i(k) - 1)$ increase with decreasing temperature. The Debye-Waller factor and the mean-square displacement were calculated from the ratios of the amplitudes at the two temperatures;

$$[k(i(k) - 1)]_{295} = \exp(-\frac{1}{2}K2\bar{d}_{\infty}^2) [k(i(k) - 1)]_{6.5}$$

The long range mean-square variation of the separation of the atoms at 295 K which is given in Table II, is denoted by \bar{d}_{∞}^2 in order to distinguish

TABLE II Thermal mean-square fluctuations excluding zero point vibrations, obtained from first and second peaks in RDF, \bar{d}_1^2 , \bar{d}_2^2 , and from Debye-Waller factor, \bar{d}_{∞}^2 , [10^{-2} \AA^2].

Temperature (K)	Te ₇₈ Si ₂₂		Te ₈₇ Si ₁₃			
	\bar{d}_1^2	\bar{d}_2^2	\bar{d}_{∞}^2	\bar{d}_1^2	\bar{d}_2^2	\bar{d}_{∞}^2
6.5	Taken to be zero					
170	0.14	1.36				
295	0.45	3.02	1.86	0.73	3.40	1.96
470	0.74	5.19				

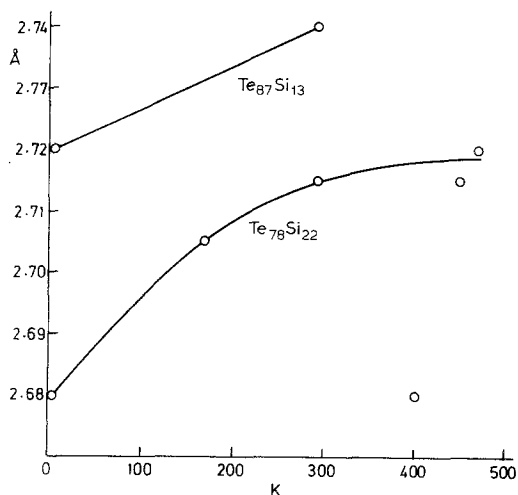


Figure 4 Position of the first peak in the RDF as function of temperature.

it from the usually different value for near neighbours. It is similar for $\text{Te}_{78}\text{Si}_{22}$ and $\text{Te}_{87}\text{Si}_{13}$ within the experimental errors. This is not surprising because above m - s variation is caused predominantly by long wavelength phonons which would not change much between 22 and 13 at. % Si. However, it is remarkable that the m - s variation for the second shell is larger than the value obtained from the Debye-Waller factor.

6. Discussion

The intersection of helical chains gives a structure for the immediate neighbourhood of Si, which fits the observations well and which is in agreement with the results of previous workers. Bartsch [2, 3] and co-workers find good agreement of the areas under the RDFs with a 4-coordinated Si and 2-coordinated Te. Although these authors did not elaborate on their models they did mention the intersection of chains as a possible structure.

Bartsch *et al.* [3] (BBJ) who measured RDFs in the concentration range 10 to 40 at. % Si, also found the shift of the first peak in the RDF to smaller distances with increasing Si content. However, their individual values are different from those given here. For 22 at. % Si BBJ give 2.62 Å in contrast to 2.715 ± 0.005 Å for the mean of 6 RDFs at 295 K which has been obtained in the present investigation. About half of this difference could be due to a difference in measurement; BBJ determined the peak position in the pair distribution function, while here the peak position in the RDF was measured. The origin of the remaining difference is not known, but as measurements with two completely different instrumentations gave 2.72 and 2.71 Å, and as no damping factor was used, the value of 2.715 Å was taken to be correct for the samples in this investigation.

The successful fit of the models to the observed RDFs allows the determination of the Si-Te and Te-Te distances separately. It can be seen from Table I that the Te-Te bond length increases from 2.74 to 2.79 with increasing Te chain length. At 13 at. % Si it has not reached the Te-Te distance in the crystal, 2.835 Å (Cherin and Unger [9]), but is equal within the experimental errors to the nearest neighbour distance in evaporated amorphous Te films, 2.79 Å (Ichikawa [10]). The Te-Te bond in amorphous Si alloys is therefore stronger than that in crystalline Te where only 26% of the total bond energy resides in the direct Te-Te bond (Grosse [11]). The Te-Si bond distance of 2.62 Å is equal to the tetrahedral Si-Te distance in crystalline Si_2Te_3 .

The results for the first peak in the RDF show that its position is not the weighted average of the Si-Te bond (2.62 Å) with the crystalline Te-Te bond (2.835 Å) as suggested by Petersen *et al.* [4], but that it is the average of the Si-Te

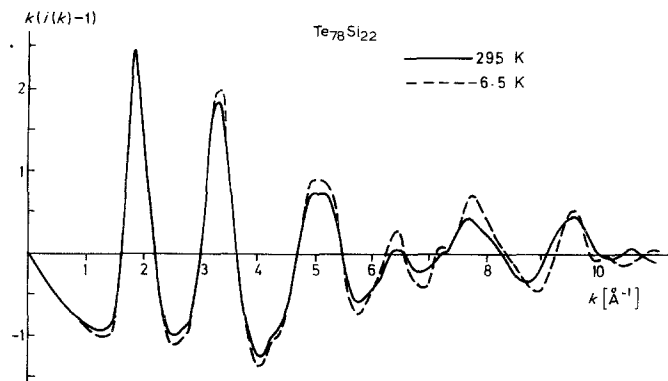


Figure 5 Temperature variation of $k(i(k)-1)$.

bond with a shortened Te–Te bond (2.74 Å for 22 at.% Si). This shortening and hence strengthening of the Te–Te bond with increasing Si concentration is to some extent reflected in the increase of the infra-red frequency of the Te–Te stretching band from 163 to 166 cm⁻¹ as observed by Bartsch *et al.* [12]. The decrease of the thermal *m*–*s* displacements (Table II) for the nearest neighbours with increasing Si concentration also supports a strengthening of the Te–Te bond. Hilton *et al.* [1] and Petersen *et al.* [4] who have investigated a variety of physical properties have reached the same conclusion: the introduction of Si strengthens the Te–Si glasses.

The *m*–*s* variation of the atomic separations which is obtained from the Debye–Waller factor can be expressed in a characteristic Debye temperature θ by

$$\overline{d_{\infty}^2} = \frac{6\hbar^2 T}{k_B m \theta^2} \phi(\theta/T)$$

where *m* is the reduced mass and ϕ the Debye function. It follows that $\theta = 230$ K for Te₇₈Si₂₂ and $\theta = 205$ K for Te₈₇Si₁₃ with an estimated error of ± 10 K. These temperatures are considerably higher than the characteristic temperature of 120 K for crystalline Te, but this is to be expected because the crystallization temperature for the Te–Si amorphous alloy is about 190 K higher than that for amorphous Te.

The *m*–*s* variation of the distance between nearest neighbours d_1^2 is less than d_{∞}^2 , giving a correlation coefficient of 0.24 and 0.37 for 22 at.% and 13 at.% Si respectively. For the second coordination shell d_2^2 is larger than d_{∞}^2 . If this is real it would demonstrate the weak nature of the Te–Te bond, because in the first shell the Si–Te bonds dominate and in the second shell the Te–Te bonds play the most important part.

From Figs. 3 and 4 it is obvious that the results for 400 and 450 K are deviating from the trend of the other measurements. This may be a real effect because the glass transition temperature is at about 433 K (Petersen *et al.* [4]) for 22 at.% Si, or it could be due to experimental error. However, the existence of these abnormalities at 400 and 450 K could not be investigated in greater detail because the instrumentation did not allow a precise control of the temperature over the large surface layer of the sample (12 mm \times 25 mm).

7. Summary

The RDFs of Te₇₈Si₂₂ and Te₈₇Si₁₃ were measured by X-ray diffraction between 6.5 and 470 K and could be fitted by a model based on the intersection of helical chains composed of Te and Si atoms. Si is tetrahedrally surrounded by Te and Te has two neighbours. Only the intersection of a right-handed helix with a left-handed helix gave a satisfactory fit to the observed RDF. This is different from the crystalline Te which has either all left or all right Te helices. The thermal *m*–*s* variations of the distances between atoms were obtained from the RDFs and from the Debye–Waller factor of the measured intensities. The actual distances together with their thermal fluctuations agree well with the structural model and with expectations based on relatively strong Si–Te bonds and weaker Te–Te bonds. From the Debye–Waller factor characteristic temperatures of 230 K (Te₇₈Si₂₂), and 205 K (Te₈₇Si₁₃), were obtained, but the errors in these, as well as in the other thermal parameters, are large and could approach ± 10 K.

Acknowledgement

The author would like to thank Professor H. Ruppertsberg for his advice during the course of this investigation, and his staff for their hospitality during the author's stay in Saarbrücken. Thanks are due to Dr H. Bromme for preparing the samples and Mr M. P. Fick for help with the low temperature measurements. The financial assistance of the Universität des Saarlandes and of the South African Council for Scientific and Industrial Research is gratefully acknowledged.

References

1. A. R. HILTON, C. E. JONES and M. BRAU, *Phys. Chem. Glasses* 7 (1966) 105.
2. G. E. A. BARTSCH and T. JUST, *Z. Metallkde* 63 (1972) 360.
3. G. E. A. BARTSCH, H. BROMME and T. JUST, *J. Non-cryst. Solids* 18 (1975) 65.
4. U. E. PETERSEN, U. BIRKHOLZ and D. ADLER, *Phys. Rev. B* 8 (1973) 1453.
5. L. G. BAILEY, *J. Phys. Chem. Solids* 27 (1966) 1593.
6. C. N. J. WAGNER in "Liquid Metals", edited by S. Z. Beer (Marcel Dekker Inc, New York, 1972 p. 258.
7. B. E. WARREN, "X-ray Diffraction" (Addison-Wesley, Reading, 1969) pp. 135–142.
8. R. J. TEMKIN, W. PAUL and G. A. N. CONNELL, *Advan. Phys.* 22 (1973) 638.

9. P. CHERIN and P. UNGER, *Acta Cryst.* 23 (1967) 670.
10. Y. ICHIKAWA, *Phys. Stat. Sol. b* 56 (1973) 707.
11. P. GROSSE, Springer Tracts in Modern Physics, Vol. 48 (Springer Verlag, Berlin, 1969) p. 15.
12. G. E. A. BARTSCH, H. BROMME and J. ZIRKE, in "The Physics of Non-Crystalline Solids" edited by

G. H Frischat, Proceedings of the 4th International conference, Clausthal-Zellerfeld (Trans. Tech., Aedermannsdorf, Switzerland, 1976) p. 591.

Received 20 December 1978 and accepted 23 March 1979.